Regulation of nuclear actin levels and MRTF/SRF target gene expression during PC6.3 cell differentiation

Kyheröinen, Salla

2022-11-15

Kyheröinen , S , Hyrskyluoto , A , Sokolova , M & Vartiainen , M K 2022 , ' Regulation of nuclear actin levels and MRTF/SRF target gene expression during PC6.3 cell differentiation ' , Experimental Cell Research , vol. 420 , no. 2 , 113356 . https://doi.org/10.1016/j.yexcr.2022.113356

http://hdl.handle.net/10138/350391
https://doi.org/10.1016/j.yexcr.2022.113356

Experimental Cell Research 420 (2022) 113356

Contents lists available at ScienceDirect

Experimental Cell Research

journal homepage: www.elsevier.com/locate/yexcr

Research article

Regulation of nuclear actin levels and MRTF/SRF target gene expression during PC6.3 cell differentiation

Salla Kyheröinen, Alise Hyrskyluoto, Maria Sokolova, Maria K. Vartiainen *

Institute of Biotechnology, University of Helsinki, Viikinkaari 5, 00014, Helsinki, Finland

A B S T R A C T

Actin has important functions in both cytoplasm and nucleus of the cell, with active nuclear transport mechanisms maintaining the cellular actin balance. Nuclear actin levels are subject to regulation during many cellular processes from cell differentiation to cancer. Here we show that nuclear actin levels increase upon differentiation of PC6.3 cells towards neuron-like cells. Photobleaching experiments demonstrate that this increase is due to decreased nuclear export of actin during cell differentiation. Increased nuclear actin levels lead to decreased nuclear localization of MRTF-A, a well-established transcription cofactor of SRF. In line with MRTF-A localization, transcriptomics analysis reveals that MRTF/SRF target gene expression is first transiently activated, but then substantially downregulated during PC6.3 cell differentiation. This study therefore describes a novel cellular context, where regulation of nuclear actin is utilized to tune MRTF/SRF target gene expression during cell differentiation.

1. Introduction

Actin is an essential protein in both the cytoplasm and nucleus, and characterized by its ability to polymerize from monomers (G-actin) to helical filaments (F-actin). In the cytoplasm, actin provides force for motile events as part of the cytoskeleton, and in the cell nucleus, actin has important roles in gene expression and maintenance of genomic integrity (reviewed in Ref. [1]). Considering the essential functions of actin in both nucleus and cytoplasm, cells must ensure appropriate regulation of protein flux between these compartments. Indeed, the nuclear and cytoplasmic pools of actin are dynamically connected, and actin shuttles rapidly in and out of the nucleus by active transport. Nuclear import of actin requires Importin-9 (Ipo9) together with the small actin-binding protein (ABP) cofilin [2], while export is carried out by Exportin-6 (Exp6) and ABP profilin [2,3]. One of the limiting factors for nuclear import and export rates is the availability of actin monomers [2,4], which depends on actin polymerization, the number of binding events with ABPs and association to larger molecular machineries, such as the chromatin remodelers.

Thus, the nucleo-cytoplasmic shuttling process of actin offers several regulatory points to tune the cellular actin balance, and alterations in nuclear actin levels have been reported in several conditions. In mammary epithelial cells, extracellular matrix component laminin-111 or lack of growth factors decrease nuclear actin levels and reduce transcription [5]. Here laminin-111 attenuates the PI3-kinase pathway, which results in Exp6 upregulation and thereby regulation of nuclear actin at the level of enhanced nuclear export. Defects in this mechanism are observed in malignant cells [6]. Nuclear actin levels are also reduced in epidermal stem cells in response to mechanical stress, with functional implications in heterochromatin anchoring, transcription and Polycomb-mediated gene silencing. Accumulation of emerin at the outer nuclear membrane and enrichment of non-muscle myosin IIA cause local actin polymerization, which decreases the available actin monomers. Hence, in this cell model, nuclear actin levels are regulated at the level of nuclear import [7]. On the other hand, *Xenopus* oocytes contain massive amounts of nuclear actin, which forms a filamentous mesh required to support the structure of these huge nuclei [8], and protect for example ribonucleoprotein droplets against gravity [9]. In these cells, nuclear actin levels seem to be regulated at the level of export, via post-transcriptional silencing of Exp6 [8] via an unknown mechanism. Increased nuclear actin levels have also been reported during differentiation of HL-60 cells towards macrophages upon PMA treatment, and binding of actin to several gene promoters is also detected in these conditions. Inhibitors targeting p38 mitogen-activated protein kinase prevent the increase in nuclear actin [10], but it is not known whether nuclear import or export of actin is affected.

Regulation of nuclear actin has also been linked to controlling transcription factor activity, and thereby to expression of specific sets of genes. Myocardin-related transcription factors (MRTFs) are co-activators of serum response factor (SRF), which regulate the expression of various cytoskeletal genes. MRTFs contain three RPEL repeats, which operate as G-actin sensors. Actin-binding inside the nucleus

* Corresponding author.
E-mail address: maria.vartiainen@helsinki.fi (M.K. Vartiainen).

https://doi.org/10.1016/j.yexcr.2022.113356
Received 14 June 2022; Received in revised form 25 August 2022; Accepted 11 September 2022
Available online 16 September 2022

promotes export of MRTF and prevents SRF activation [11] and abundant cytoplasmic G-actin also inhibits MRTF nuclear import [11–13]. Importantly, since actin itself, as well as many ABPs, are transcriptional targets of MRTF/SRF, this creates a feedback loop, where actin dynamics control the expression of proteins driving actin dynamics. Several mechanisms that culminate on nuclear actin have been reported to regulate MRTF/SRF-dependent gene expression. Serum stimulation and cell spreading cause transient polymerization of nuclear actin via mDia formins, leading to MRTF nuclear accumulation and SRF activation [14,15]. Another MRTF/SRF activating protein is MICAL-2, an atypical actin regulator that localizes to the nucleus and induces redox-dependent actin filament depolymerization, thus lowering nuclear G-actin levels

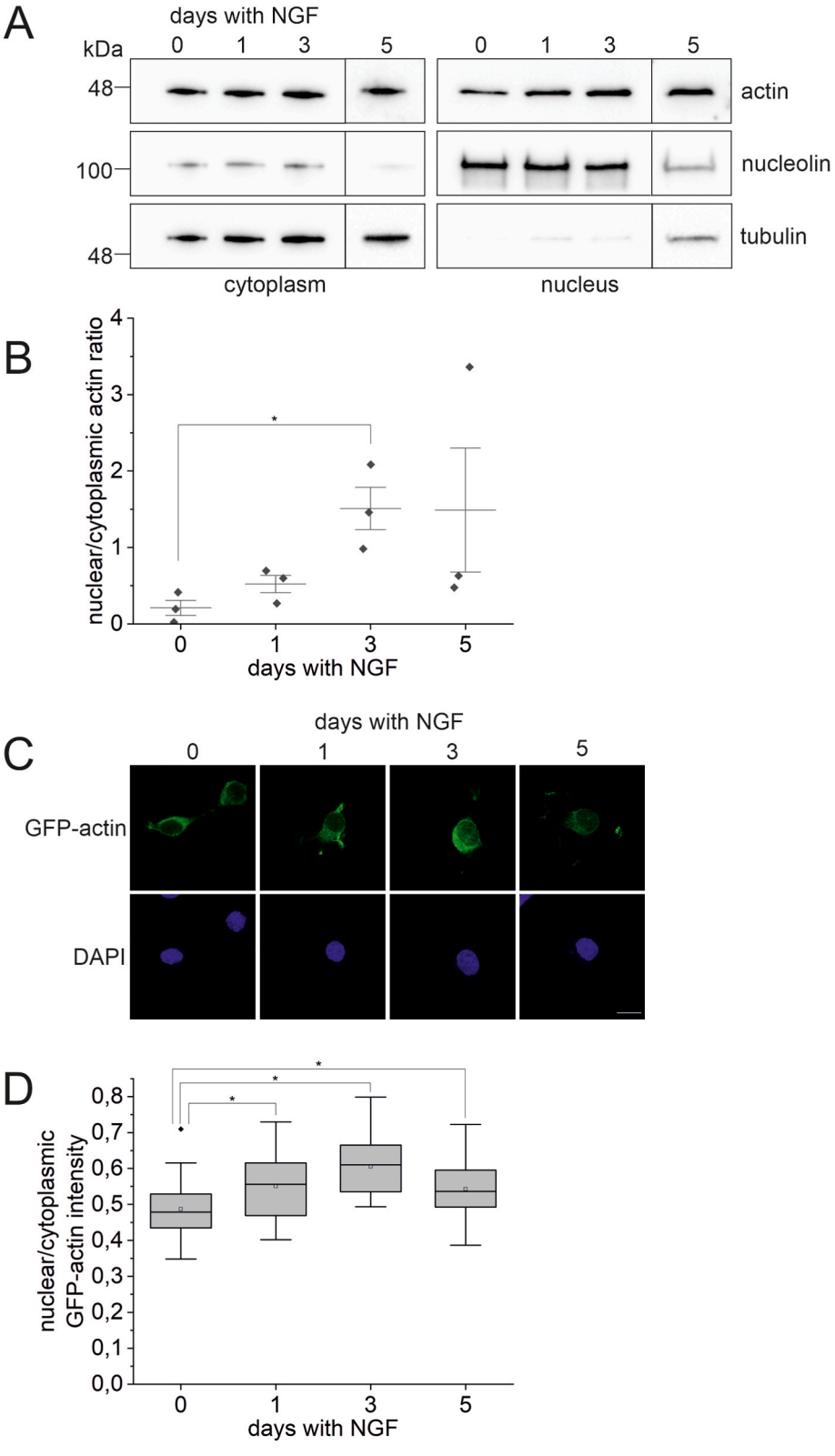

Fig. 1. Nuclear actin levels increase during PC6.3 differentiation. A. Western blotting with indicated antibodies of nuclear and cytoplasmic protein fractions from PC6.3 cells differentiated for 0, 1, 3 or 5 days with NGF. Tubulin used as cytoplasmic and nucleolin as nuclear markers. Molecular weights based on markers are indicated on the left. Boxed areas are from separate Western blots. B. Quantification of nuclear to cytoplasmic actin distribution from Western blots. Data is shown as a scatter interval plot, with individual measurements (N = 3) shown as black dots, error bars ± 0.5 standard deviation (SD) and mean as the horizontal line. * Statistically significant differences ($P < 0.05$) with a two-sample *t*-test: 0 vs. 1 day P = 0.146, 0 vs. 3 days P = 0.042, 0 vs. 5 days P = 0.305. C. Confocal microscopy images of PC6.3 cells transfected with GFP-actin and differentiated for 0, 1, 3 or 5 days. Nuclei stained with DAPI. Scale bar 10 μm. D. Quantification of GFP-actin distribution between nucleus and cytoplasm during PC6.3 cell differentiation. Data is shown as a box plot, where boxes represent 25%–75% of the values and error bars the range within 1.5IQR. Middle line is the median, open square is the mean, and black dots are outliers. $N \geq 20$ cells measured per condition. * Statistically significant differences ($P < 0.05$) with a two-sample *t*-test: 0 vs. 1 day P = 0.039, 0 vs. 3 days P = 3.162E-5 and 0 vs. 5 days P = 0.035. See also Fig. S1.

[16]. On the other hand, Ras association domain family 1 isoform A (RASSF1A) regulates nuclear actin levels, and thereby MRTF/SRF activity, by promoting the association between Exp6 and Ran GTPase. *Rassf1a* is silenced by promoter hypermethylation in many solid tumors, and cancer cells defective in this pathway display increased nuclear actin, reduced MRTF activity and consequent defects in cell adhesion [17]. However, also activation of MRTF/SRF target genes have been reported in malignant cells to promote invasiveness. Nuclear capture of receptor tyrosine kinase EphA2-containing endosomes activates RhoG, which promotes phosphorylation of cofilin, decreased nuclear G-actin levels, and thereby activation of MRTF/SRF target gene expression [18]. In vascular smooth muscle cells, elevated cAMP signaling increases the availability of cytoplasmic actin monomers, which are then transported into the nucleus, where they in turn inhibit YAP-TEAD and MRTF/SRF activity [19]. Thus, many mechanisms exist to regulate different aspects of nuclear actin from its levels to polymerization in order to control MRTF/SRF transcriptional activity.

Here we describe a novel cellular context, where nuclear actin levels are regulated to influence MRTF/SRF target gene expression. By using PC6.3 cells as an *in vitro* model for neuronal differentiation, we demonstrate that MRTF/SRF target gene expression is first rapidly activated, but then significantly repressed during the differentiation process. Repression of MRTF/SRF activity takes place at the level of MRTF-A subcellular localization, and coincides with increased nuclear actin levels due to decreased nuclear export of actin.

2. Results

2.1. Nuclear actin levels increase during PC6.3 cell differentiation

In this study, we use PC6.3 cells as an *in vitro* cell differentiation model. PC6.3 cells are a subclone of the rat PC12 pheochromocytoma cell line, and widely used to study the different pathways controlling neuronal differentiation and how factors, such as chemicals, affect neurite outgrowth. Treatment of PC6.3 cells with neural growth factor (NGF) ceases their proliferation, induces neurite outgrowth (Fig S1A) and the cells acquire properties of sympathetic neurons. Differentiation is induced through the TrkA receptor and initiates several signaling cascades [20]. Differentiation of PC6.3 cells can be easily followed by monitoring the number and length of neurites (Fig S1A), and by

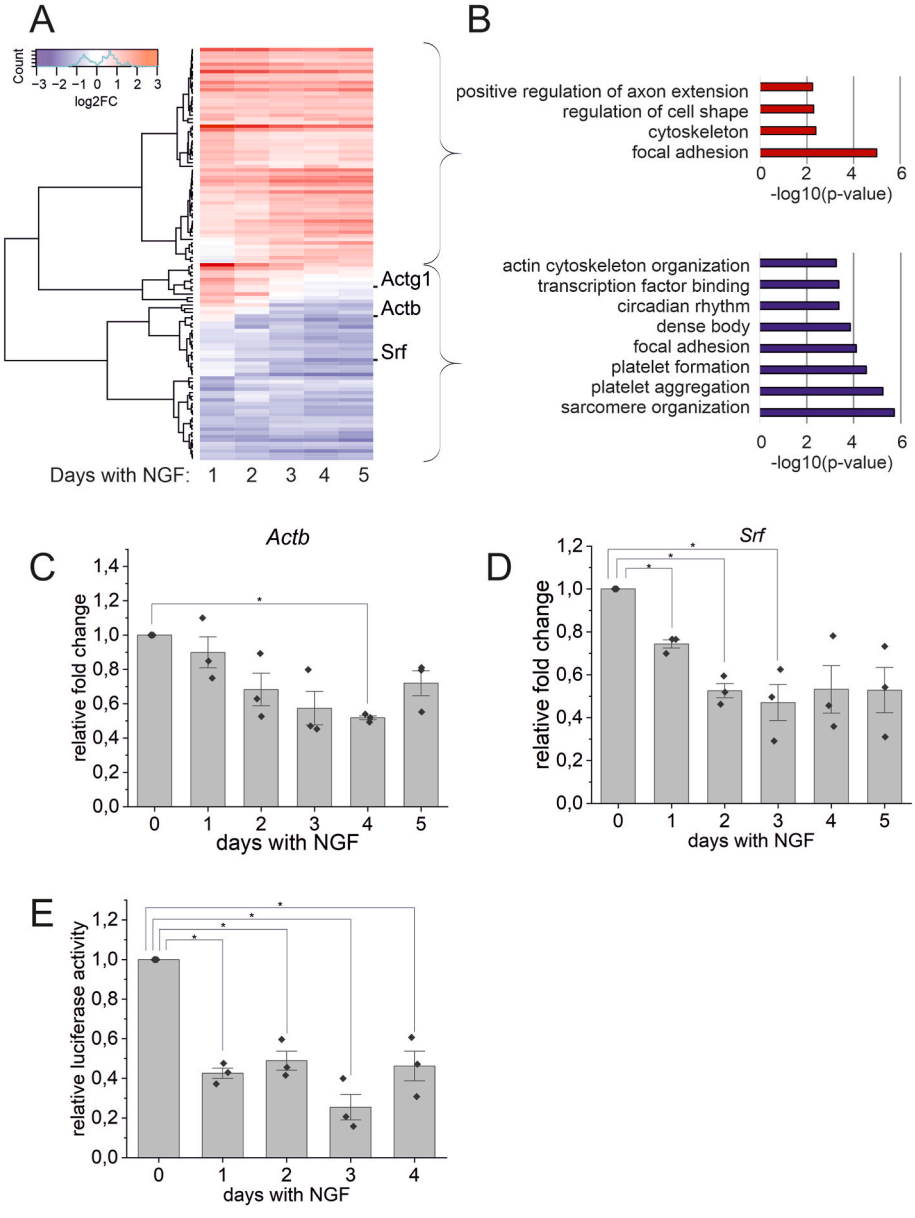

Fig. 2. RNA-seq reveals decreased expression of MRTF/SRF target genes upon PC6.3 cell differentiation. A. Heatmap showing relative expression of MRTF-A direct target genes [23], which display at least 50% change in their expression during differentiation (log2FC < −0.6 and log2FC > 0.6; N = 113) compared to undifferentiated cells. Canonical MRTF/SRF target genes indicated on the right. B. Gene Ontology enrichment analysis of MRTF-A direct target genes (see A) with increased (top) and decreased (bottom) relative expression during differentiation. C. qPCR of *Actb* during 0–5 days of differentiation normalized to undifferentiated control sample. Data is mean (N = 3), error bars SD, individual measurements shown as black dots. * Statistically significant differences (P < 0.05) with a one-sample *t*-test: 0 vs. 1 day P = 0.436, 0 vs. 2 days P = 0.101, 0 vs. 3 days P = 0.063, 0 vs. 4 days P = 7.827E-4, 0 vs. 5 days P = 0.079. D. qPCR of *Srf* (N = 3) during 0–5 days of differentiation normalized to undifferentiated control sample; data shown as in C. * Statistically significant differences (P < 0.05) with a one-sample *t*-test: 0 vs. 1 day P = 0.007, 0 vs. 2 days P = 0.006, 0 vs. 3 days P = 0.032, 0 vs. 4 days P = 0.067, 0 vs. 5 days P = 0.061. E. Relative SRF luciferase activity in PC6.3 cells differentiated for 0–4 days. Data is shown as mean (N = 3), normalized to undifferentiated control sample, error bars SD and individual measurements shown as black dots. * Statistically significant differences (P < 0.05) with a one-sample *t*-test: 0 vs. 1 day P = 0.003, 0 vs. 2 days P = 0.011, 0 vs. 3 days P = 0.010, 0 vs. 4 days P = 0.025. See also Fig S2.

measuring the induction of several target genes [21,22]; see below Fig. 2 for RNA-seq data. Differentiation is visible already 24 h after NGF addition [24] and reaches a plateau after 6 days [25]. Here we follow differentiation until 5 days after NGF treatment.

To study, if nuclear actin levels respond to PC6.3 differentiation we used cell fractionation (Fig. 1A–B) and imaging approaches (Fig. 1C–D). Cell fractionation revealed a significant increase in nuclear actin amounts after 3 days of differentiation. The levels were still elevated at 5 days of NGF treatment, but the variation was greater at later time points (Fig. 1B). Similar observations were made by using fluorescence microscopy to quantify the distribution of GFP-actin between the nucleus and cytoplasm (Fig. 1C–D). The ratio of nuclear to cytoplasmic GFP-actin intensity was the highest after 3 days of NGF treatment, and GFP-actin remains more nuclear at day 5 compared to untreated cells (Fig. 1D). Western blotting of total actin levels revealed that the amount of actin decreases during PC6.3 cell differentiation and at day 4, the decrease is statistically significant (Fig S1B-C). This indicates that the increased nuclear actin is not due to overall increase in the amount of cellular actin, but rather reflects regulation of the subcellular distribution of actin. This idea is also supported by the results from GFP-actin localization (Fig. 1C–D), which is not dependent on endogenous actin expression. Taken together, nuclear actin levels are subject to regulation during PC6.3 cell differentiation, reaching the peak level at 3 days after NGF addition.

2.2. Reduced expression of MRTF/SRF target genes during PC6.3 cell differentiation

To explore the possible functional implications of increased nuclear actin levels during PC6.3 cell differentiation, we used RNA-sequencing (RNA-seq) to analyze changes in gene expression levels. RNA-seq was performed in four biological replicates from undifferentiated cells and cells treated with NGF for 1–5 days. Principal component analysis reveals that the largest differences in gene transcription take place during the first day of differentiation (Fig S2A). Analysis of the 12 872 expressed genes (baseMean expression levels above 10) by comparing their expression to undifferentiated cells (log2FC) during NGF treatment (Supplementary Table S1) identifies different classes of transcriptional responses during PC6.3 cell differentiation (Fig S2B). These classes include, for example, genes that are either up- or downregulated already from the first day of differentiation (clusters I-IV and V-VII, respectively, of Fig S2B), and those that show a more complex expression pattern, such as initial upregulation at day 1 of NGF treatment, followed by downregulated expression at subsequent days of differentiation (cluster IV and partially cluster VI of Fig S2B, see also below). In agreement with previous gene expression analysis of PC6.3 and the related PC12 cells [21,22,26], the genes upregulated already during the first day of NGF treatment (335 genes with logFC>1) contain many genes implicated in neuronal differentiation (for example GO terms nervous system development, P-value = 0.0011; myelin sheath, P-value = 0.0001; Supplementary table S2). Many of these genes, including *Syn2*, *Ngef, Nefm* and *Thy1*, remain upregulated until day 5 (209 from 335 with logFC>1 on day 1 and day 5). In addition to neuronal differentiation, the upregulated genes are also enriched for GO terms related to plasma membrane remodeling (Supplementary table S2), likely reflecting the need to remodel the cell surface for neurite extension. On the other hand, genes that display reduced expression already after 1 day of NGF treatment are linked to processes of cell division (for example GO terms cell division P-value = 1.8E-13; chromosome segregation P-value = 7.70E-12) in line with ceased proliferation during PC6.3 cell differentiation [27]. Overall, these results reflect the cellular processes known to take place during PC6.3 cell differentiation, and are in line with previous gene expression analysis in similar experimental systems [21,22].

Among the genes that were downregulated at day 5 compared to day 1 of differentiation (Supplementary Table S2), we recognized several well-established target genes of MRTF/SRF, including for example *Actb*. Since nuclear actin has been shown to regulate MRTF/SRF transcriptional activity in several experimental systems, we decided to analyze expression of these genes in more detail. In the absence of an established target gene list for MRTF/SRF in neuronal cells, we utilized data from mouse fibroblasts, where MRTF target genes were defined based on binding of MRTF-A to these genes by ChIP-seq and their sensitivity to actin-binding drugs known to influence MRTF activity [23]. Of the 467 MRTF targets, 113 genes displayed at least 50% change in their expression during differentiation (Fig. 2A and B; Supplementary table S3; based on the log2FC < -0.6 and log2FC > 0.6 compared to non-treated cells). Of these genes, 46 were upregulated and 14 were downregulated at day 1 of NGF treatment. At day 3 of NGF treatment, there were 41 upregulated and 21 downregulated, and at day 5, 45 upregulated and 32 downregulated MRTF target genes, when compared to undifferentiated conditions. Thus, the number of downregulated MRTF target genes increased during PC6.3 cell differentiation. Moreover, majority (34 of 46) of the initially upregulated target genes displayed decreased expression, when comparing the day 5 to the day 1 of differentiation. This indicates that even though some MRTF/SRF target genes are initially activated during PC6.3 cell differentiation, there is an overall trend towards downregulating this pathway.

To confirm decreased MRTF/SRF target gene expression, we performed qPCR analysis of selected target genes during 0–5 days of NGF treatment. In agreement with RNA-seq, the expression of *Actb* (Fig. 2C) mRNA was decreasing during PC6.3 cell differentiation and is in line with total actin protein levels (Fig S1B-C). Also expression of *Srf* mRNA was downregulated from the first day of differentiation (Fig. 2D). However, Western blotting of SRF protein levels did not reveal statistically significant changes (Fig S2C-D), although the trend was the same as observed for mRNA (Fig. 2D). This indicates that the decreased expression of *Srf* mRNA is not sufficient to significantly alter SRF protein levels in this experimental set-up. Finally, we investigated the SRF transcriptional activity with a reporter assay in differentiating PC6.3 cells. In agreement with RNA-seq and qPCR data, SRF reporter activity declined already during the first day of differentiation, and the decrease continued towards day 4 of differentiation (Fig. 2E).

Based on the RNA-seq data, some MRTF/SRF target genes were upregulated during the first day of differentiation, but then their expression declined from the second day of NGF treatment (Fig. 2A–B). Due to this observation, and since previous studies have reported upregulation of SRF activity during the first hours of PC12 cell differentiation [26], we decided to study also earlier time points during the first day of NGF treatment. Indeed, we observed increased SRF reporter gene activity after 8 h of NGF stimulation compared to undifferentiated cells (Fig. 3A). Moreover, qPCR analysis revealed that transcription of both *Srf* (Fig. 3B) and *Vcl* (Fig. 3C) were activated during the first hours of NGF stimulation. Especially *Srf* expression rapidly decreased back to baseline expression levels after peaking at 2 h of NGF stimulation (Fig. 3B), while *Vcl* expression remained elevated for longer time (Fig. 3C). Taken together, our RNA-seq, qPCR and SRF reporter gene assays reveal that MRTF/SRF-mediated transcription is tightly regulated during PC6.3 cell differentiation. During the first hours of NGF-induced differentiation, expression of MRTF/SRF target genes is transiently activated, but then the pathway is repressed.

2.3. Subcellular localization of MRTF-A is subject to regulation during PC6.3 cell differentiation

Next, we wanted to understand the cellular processes that lead to regulation of MRTF/SRF target genes during PC6.3 cell differentiation. Since SRF protein levels were not significantly reduced during the process (Fig S2C-D), it is unlikely to fully explain reduced expression of its target genes. We therefore turned our attention to MRTF cofactors. RNA-seq did not reveal significant changes in *Mrtf-a* expression (Supplementary Table S1), and also Western blotting with antibody recognizing MRTF-A failed to reveal consistent changes in protein levels during 0–5

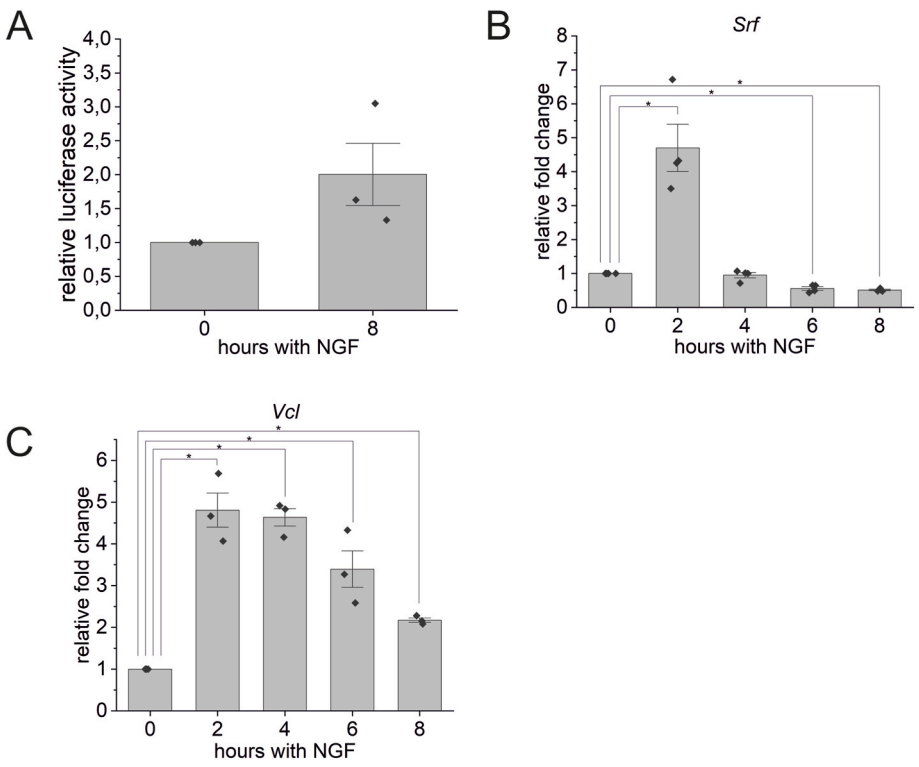

Fig. 3. Increased MRTF/SRF transcriptional activity at early time points of NGF stimulation. A. Relative SRF luciferase activity in PC6.3 cells treated or not for 8 h with NGF. Data is shown as mean (N = 3), normalized to untreated sample, error bars SD and individual measurements shown as black dots. 0 vs. 8 h P = 0.199 with one-sample *t*-test. B. qPCR of *Srf* during 0–8 h of differentiation. Data is shown as mean (N = 4), normalized to undifferentiated control sample, error bars SD, individual measurements shown as black dots. * Statistical significance (P < 0.05) with a one-sample *t*-test 0 vs. 2 h P = 0.013, 0 vs. 4 h P = 0.564, 0 vs. 6 h P = 0.004, 0 vs. 8 h P = 1.427E-4. C. qPCR of *Vcl*, shown as in B, (N = 3). * Statistical significance (P < 0.05) with a one-sample *t*-test: 0 vs. 2 h P = 0.015, 0 vs. 4 h P = 0.004, 0 vs. 6 h P = 0.042, 0 vs. 8 h P = 0.002.

days of PC6.3 cell differentiation, apart from a transient increase in MRTF-A expression at day 1 (Fig. 4A–B). It is well established in fibroblasts that nuclear actin regulates subcellular localization of MRTF-A [11,14], but the nucleo-cytoplasmic shuttling process of MRTF in neuronal cells seems to be cell-type specific [28]. We therefore used immunofluorescence staining of MRTF-A to study its subcellular localization during PC6.3 cell differentiation. In agreement with target gene expression (Fig 2A, C-E and Fig. 3), MRTF-A was translocated from the cytoplasm to the nucleus already after 30 min of NGF treatment, but then its localization returned to almost baseline at 2 h of NGF (Fig. 4C–D). Experiments with longer time points revealed reduced nuclear MRTF-A compared to untreated cells from day 3 of differentiation (Fig. 4E–F). Taken together, MRTF-A subcellular location is tightly regulated during PC6.3 cell differentiation. During the first hours of differentiation, MRTF-A transiently accumulates in the nucleus and then returns back to baseline. Around day 3 of differentiation, the nuclear levels of MRTF-A are even further reduced. This localization data fits very well with MRTF/SRF target gene expression, and repression of the pathway coincides with increased nuclear actin levels, in agreement with data from other cellular systems with elevated nuclear actin [17,19].

2.4. Reduced nuclear export of actin upon PC6.3 cell differentiation

We have previously shown that nuclear actin levels are actively maintained by nuclear transport [2]. Thus, the increase in nuclear actin levels observed during PC6.3 cell differentiation can be due to either increased nuclear import or decreased nuclear export of actin. To study this, we used different photobleaching methods to measure nuclear transport of GFP-actin [29]. These assays were performed until day 3 of differentiation, when the actin accumulation in the nucleus seems to peak. First, we studied nuclear import of actin with fluorescence recovery after photobleaching (FRAP) assay. Here, the nucleus is bleached once with full laser power, and the recovery of nuclear fluorescence, due to import of unbleached GFP-actin molecules, is followed. As described before [2], the beginning of the recovery curve gives a good measure of the nuclear import rate, but later nuclear export will start to influence fluorescence recovery. Overall, the shape of the recovery curve was very similar in cells differentiated for 0, 1 and 3 days (Fig. 5A), and also the import rate between different days did not show significant changes (Fig. 5B). We note that the average fluorescence recovery curve for the cells treated for 1 day with NGF shows somewhat higher initial fluorescence levels, which may reflect subtle differences in overall actin mobility in this sample.

Our previous research has demonstrated that nuclear import of actin is dependent on Ipo9 and cofilin, in its unphosphorylated form [2]. To study the abundance of these molecules during PC6.3 cell differentiation, we used Western blotting (Fig. 5C). However, we did not observe any significant changes in either Ipo9 protein levels (Fig. 5D), or the ratio between phospho-cofilin and cofilin (Fig. 5E). The total levels of cofilin are slightly higher during the first days of differentiation (Fig S5A), but these changes are not statistically significant. Furthermore, this applies also to phospho-cofilin (Fig S5B). Moreover, based on RNA-seq data (Supplementary table S1) neither *Ipo9* nor *Cfl* mRNAs displayed significant changes in their expression levels during PC6.3 cell differentiation. This was further confirmed for *Ipo9* using qPCR (Fig S5C). Combined, these experiments did not show any significant changes in nuclear import rate of actin (Fig. 5B) or in the abundance of proteins required for this process (Fig. 5D–E). This suggests that nuclear import of actin is not the regulatory step driving increased nuclear actin levels during PC6.3 cell differentiation.

Next, we studied nuclear export of actin with fluorescence loss in photobleaching (FLIP) assay, where cytoplasm is continuously bleached, and loss of nuclear fluorescence, due to nuclear export of GFP-actin, is measured [2,29]. This assay revealed clear differences especially at 3 days of NGF treatment compared to untreated cells (Fig. 6A–C). Nuclear export rate, plotted from the initial loss of fluorescence, was significantly slower at 3 days of NGF treatment compared to untreated cells (Fig. 6B). We also note that the export rates were clearly less variable in differentiated cells compared to undifferentiated. Moreover, there was significantly more GFP-actin fluorescence remaining in the nucleus after 100 s of bleaching already in the cells treated for 1 day with NGF, and

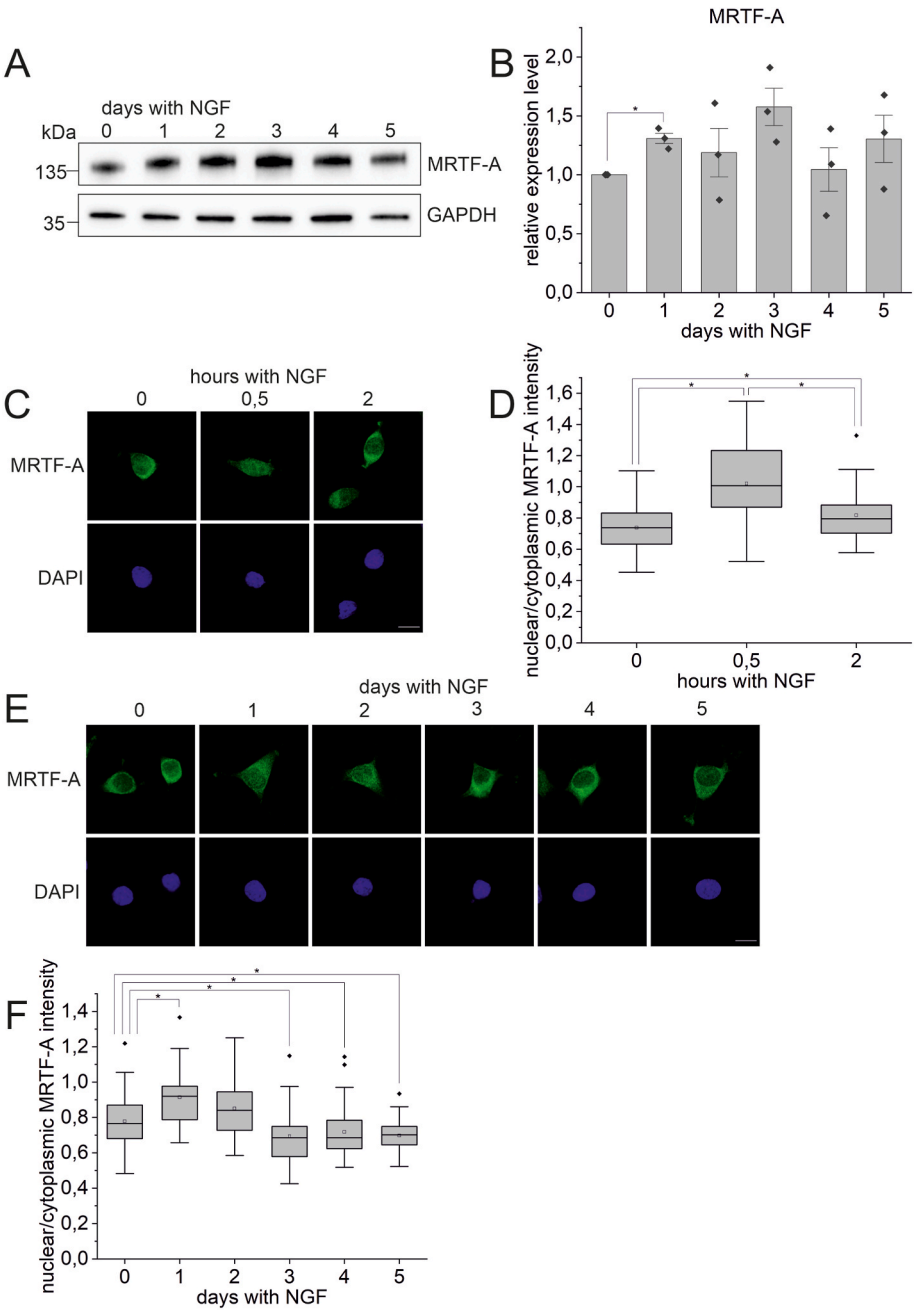

Fig. 4. MRTF-A nuclear localization is regulated during PC6.3 cell differentiation. A. Western blotting of total MRTF-A protein levels during PC6.3 cell differentiation at indicated days with NGF. GAPDH used as the loading control. Note that GAPDH is the same as in Fig S2C. B. Quantification of MRTF-A levels from Western blots. Data is mean (N = 3), normalized to undifferentiated sample, error bars SD, individual data points shown as black dots. * Statistically significant differences ($P < 0.05$) with a one-sample *t*-test. 0 vs. 1 day P = 0.025, 0 vs. 2 days P = 0.510, 0 vs. 3 days P = 0.088, 0 vs. 4 days P = 0.854, 0 vs. 5 days P = 0.320. C. Confocal microscopy images of cells differentiated for 0–2 h and stained with anti-MRTF-A antibody. Nuclei stained with DAPI. Scale bar 10 μm. D. Quantification of MRTF-A nuclear to cytoplasmic distribution from microscopy images. Data is shown as a box plot, where boxes represent 25%–75%, middle line is the median, open square is the mean, black dots are the outliers and error bars show the range within 1.5IQR. N ≥ 36 cells measured per condition. * Statistically significant differences ($P < 0.05$) with a Mann-Whitney test: 0 vs. 0.5 h P = 1.687E-7, 0 vs. 2 h P = 0.011, 0.5 vs. 2 h P = 1.613E-4. E. Confocal microscopy images of cells differentiated for 0–5 days and stained with anti-MRTF-A and DAPI. Scale bar 10 μm. F. Quantification of MRTF-A nuclear to cytoplasmic distribution. Data is shown as in D; N ≥ 30 cells measured per condition. * Statistically significant differences ($P < 0.05$) with a Mann-Whitney test: 0 vs. 1 day P = 0.001, 0 vs. 2 days P = 0.065, 0 vs. 3 days P = 0.012, 0 vs. 4 days P = 0.046, 0 vs. 5 days P = 0.021.

the effect was even more pronounced at day 3 (Fig. 6C). In addition to the nuclear export rate, the portion of GFP-actin remaining in the nucleus at the end of the assay represents the availability of export competent actin monomers [2]. Our results therefore suggest that in differentiated cells, actin might be more polymerized or tightly bound to nuclear complexes, such as chromatin remodelers, than in undifferentiated cells. Since our data clearly indicates decreased nuclear export of actin in differentiated PC6.3 cells compared to undifferentiated cells, studies on Exp6 protein levels would have been very interesting. However, we failed to identify an antibody that would have specifically detected Exp6 protein from the rat cells used for this study. Due to the strict cut-off *Xpo6* was not among the differentially expressed genes in the RNA-seq dataset (Supplementary table S1). Nevertheless, qPCR analysis revealed moderate decrease in *Xpo6* mRNA levels during PC6.3 cell differentiation (Fig. 6D), which is in line with the RNA-seq data (for example at day 3, log2FC = −0.35 with P-value = 0.0000002 compared to undifferentiated cells). Whether this decrease is sufficient to impact Exp6 protein levels, and thereby nuclear export of actin, warrants the development of new reagents.

3. Discussion

The cellular actin balance is maintained by active nucleocytoplasmic shuttling that is subject to regulation at different levels to control the relative abundance of actin in the nuclear and cytoplasmic compartments. Indeed, regulation of nuclear actin levels have been reported during various cellular processes, from differentiation to disease [30]. Functionally, alterations in nuclear actin levels are most often linked to either gene-specific transcriptional regulation or overall transcriptional activity. Nevertheless, neither the signaling pathways nor the mechanisms by which increased or decreased nuclear actin levels influence transcription are fully understood. Here we extend the studies on

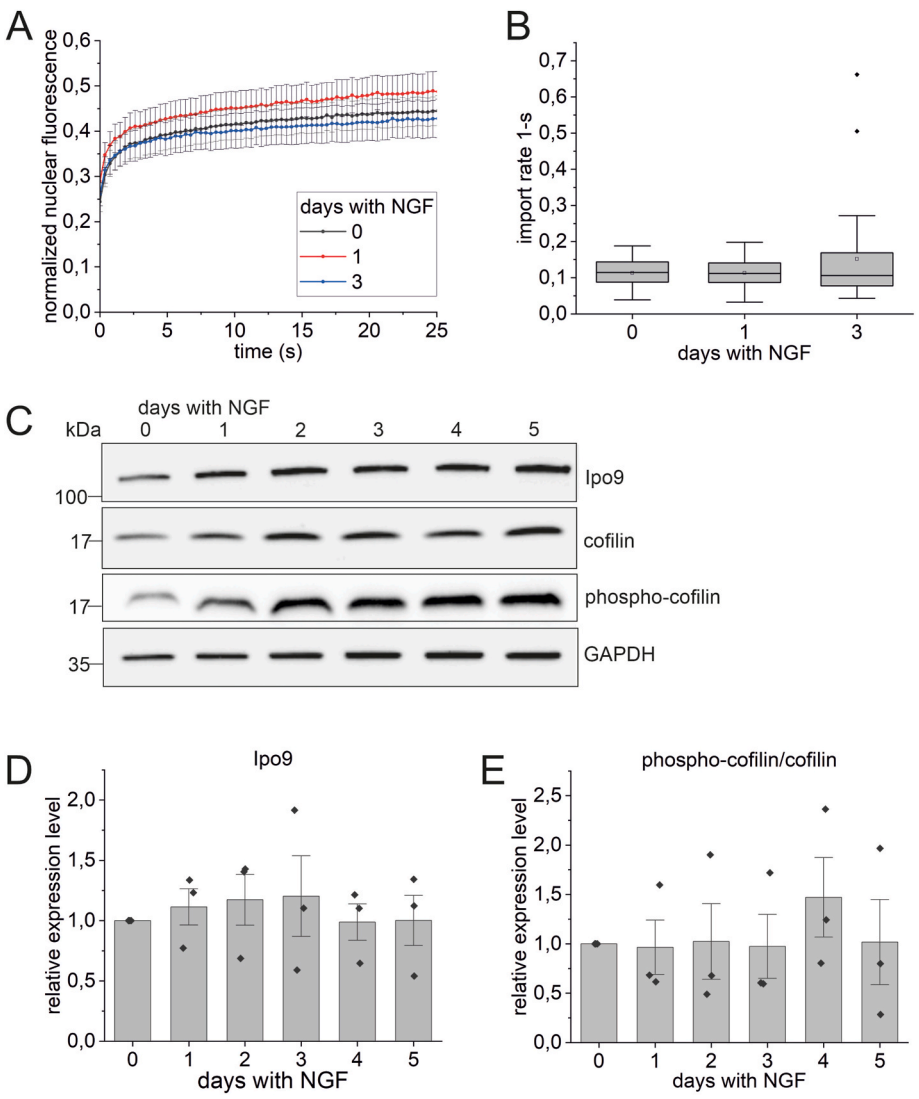

Fig. 5. Nuclear import of actin is not affected during PC6.3 cell differentiation. A. Fluorescence recovery curves from FRAP assay representing nuclear import of fluorescent actin molecules in cells differentiated for indicated days with NGF. Data is mean (N ≥ 27 cells measured per condition), normalized to pre-bleach values, error bars SD. B. Apparent nuclear import rate of GFP-actin from FRAP assay in cells differentiated for indicated days with NGF. Data is shown as a box plot, where boxes represent 25%–75%, middle line is the median, open square the mean, error bars represent the range within 1.5IQR and black dots are the outliers. Statistical significance with a Mann-Whitney test: 0 vs. 1 day P = 0.885, 0 vs. 3 days P = 0.997. C. Western blot of Ipo9, cofilin and phospho-cofilin levels during PC6.3 differentiation for indicated days. GAPDH used as the loading control. All proteins blotted from the same sample set. Molecular weights on the left. D. Quantification of Ipo9 Western blots. Data is mean (N = 3), normalized to undifferentiated sample, error bars SD and individual data points shown as black dots. Statistical significance with a one-sample *t*-test 0 vs. 1 day P = 0.578, 0 vs. 2 days P = 0.550, 0 vs. 3 days P = 0.651, 0 vs. 4 days P = 0.950, 0 vs. 5 days P = 0.994. E. Quantification of phospho-cofilin/cofilin levels from Western blots. Data (N = 3) is shown as in D. Statistical significance with a one-sample *t*-test: 0 vs. 1 day P = 0.923, 0 vs. 2 days P = 0.963, 0 vs. 3 days P = 0.950, 0 vs. 4 days P = 0.418, 0 vs. 5 days P = 0.976. See also Fig S5.

nuclear actin regulation by demonstrating that nuclear actin levels increase upon PC6.3 cell differentiation towards neuron-like cells (Fig. 1). This increase is due to reduced nuclear export of actin during differentiation (Fig. 6). Gene expression analysis reveals that MRTF/SRF target gene expression is first transiently activated (Fig. 3), but then substantially downregulated during PC6.3 cell differentiation (Fig. 2). This study therefore provides novel insights into nuclear actin regulation and MRTF/SRF pathway in a cellular differentiation model.

The nucleo-cytoplasmic shuttling process of actin offers several regulatory points to influence the cellular actin balance [2]. Indeed, previous studies have revealed regulation at the level of both nuclear import [7] and export [6,8], and through regulation of either nuclear transport factors [6] or actin itself [7]. By using photobleaching assays to measure nuclear transport rates of actin, we show that in PC6.3 cells, actin is regulated at the level of nuclear export (Fig. 6A–C), but not nuclear import (Fig. 5A–B). Reduced export could be achieved by modulating either the levels and/or activity status of the proteins needed for nuclear export of actin, or by regulating the availability of transport competent actin. Our fluorescence loss in photobleaching experiments reveal both decreased export rate of actin (Fig. 6B) and increased retention of actin in nucleus (Fig. 6C). These two processes are obviously linked, but the FLIP assay used here does not allow us to differentiate between them. In *Xenopus* oocytes, the massive nuclear actin amount that gives rise to a filamentous meshwork is achieved by post-transcriptional downregulation of Exp6 protein levels [8]. Our qPCR results suggest a modest decrease in *Xpo6* mRNA levels during PC6.3 cell differentiation (Fig. 6D). However, our failure to identify an antibody that would reliably recognize rat Exp6 protein prevented further studies on this topic. RASSF1A is required for nuclear export of actin by supporting the interaction between Exp6 and the Ran GTPase, and its expression levels are regulated by promoter hypermethylation in several solid tumors [17]. However, our RNA-seq analysis did not reveal significant changes in *Rassf1* during PC6.3 cell differentiation (Supplementary table S1). In mouse epithelial cells, attenuation of the PI3-kinase activity enhances nuclear export of actin [6], but the mechanism has remained unclear. Interestingly, NGF seems to stimulate PI3K activity during PC6 and PC12 cell differentiation [31,32], and the PI3K inhibitor LY294002 inhibits NGF-induced neurite outgrowth [33]. It is therefore tempting to speculate that enhanced PI3K activity during PC6.3 differentiation reduces nuclear export actin and leads to the observed accumulation of nuclear actin. Another signaling pathway that could play a role is the MAP kinase pathway, which is also activated downstream of NGF [34]. Upon differentiation of HL-60 cells towards macrophages, treatment with MAP kinase inhibitors prevents nuclear accumulation of actin [10]. Development of new tools to study the Exp6 protein is required to explore these possibilities further.

Actin monomer levels can limit nuclear transport rates of actin [2] and our FLIP assay hinted that less actin might be available for nuclear

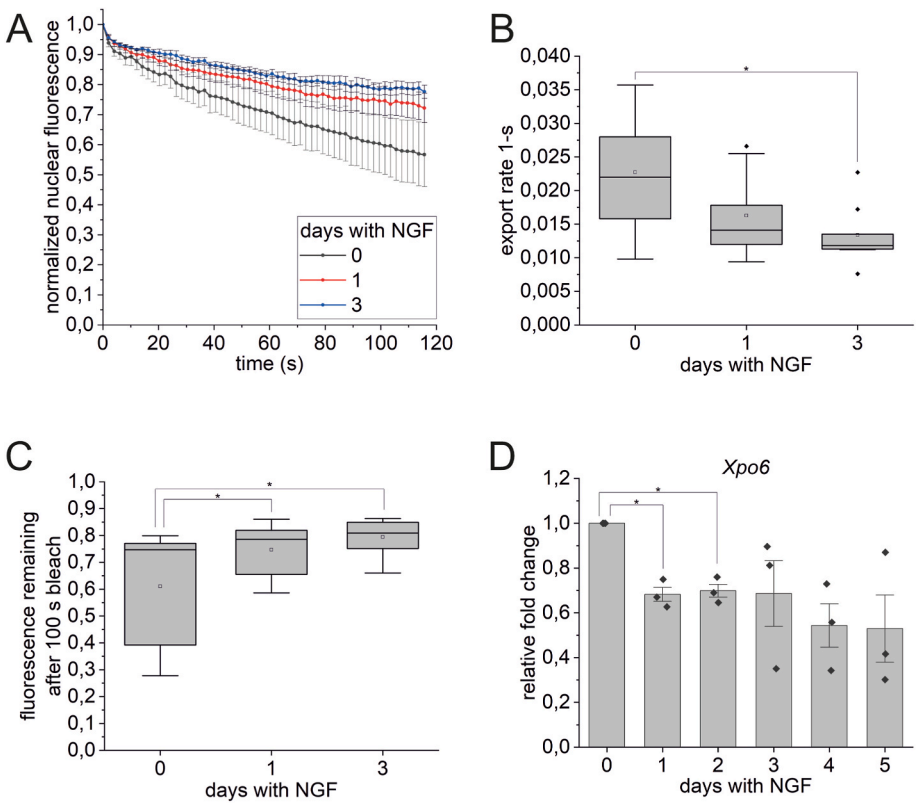

Fig. 6. Slower nuclear export of actin during PC6.3 cell differentiation. A. Fluorescence loss curves from FLIP assay representing nuclear export of actin molecules in cells differentiated for indicated days with NGF. Data is mean ($N \geq 11$ cells per condition), normalized to pre-bleach frames and error bars SD. B. Nuclear export rate of GFP-actin quantified from FLIP assay. Data is shown as a box plot, where boxes represent 25%–75%, middle line is the median, open square the mean, error bars represent the range within 1.5IQR and black dots are the outliers. * Statistically significant differences ($P < 0.05$) with a two-sample *t*-test: 0 vs. 1 day $P = 0.092$, 0 vs. 3 days $P = 0.014$. C. Fluorescence remaining after 100 s bleach in the FLIP assay. Data is shown as a box plot as in B. * Statistically significant differences ($P < 0.05$) with a Mann-Whitney test: 0 vs. 1 day $P = 0.027$, 0 vs. 3 days $P = 0.003$. D. qPCR of *Xpo6* mRNA ($N = 3$) during PC6.3 cell differentiation. Data is shown as mean ($N = 3$), normalized to undifferentiated control sample, error bars SD and individual data points shown as black dots. * Statistically significant differences ($P < 0.05$) with a one-sample *t*-test: 0 vs. 1 day $P = 0.013$, 0 vs. 2 days $P = 0.012$, 0 vs. 3 days $P = 0.206$, 0 vs. 4 days $P = 0.055$, 0 vs. 5 days $P = 0.113$.

export in differentiated PC6.3 cells (Fig. 6C). This could arise either from increased nuclear polymerization of actin or from actin-binding to nuclear complexes. We did not observe clear phalloidin staining in the nuclei of PC6.3 cells in any condition (data not shown). Moreover, nuclear actin polymerization is most often linked to activation of MRTF/SRF target gene expression [14,15], which is contrary to what we observe here in PC6.3 cells (Fig 2A, C-D). Since actin is an essential component of chromatin remodelers [35] and also needed to sustain maximal transcription [2,36] it can be speculated that these roles become more important during differentiation, requiring more actin to be associated with these complexes. This could explain increased retention of actin during PC6.3 cell differentiation. It is indeed known that during differentiation, thousands of genes are repositioned inside the nucleus and these relocations are driven by chromatin remodeling and correlate with changes in transcription and replication timing [37]. Actin could be one possible candidate to regulate these global changes in chromatin organization during differentiation. Indeed, mouse embryonic fibroblasts (MEFs) lacking the β-actin gene display altered 3D genome architecture [38] and are defective in their reprogramming capacity towards osteoblast-like cells [39], adipocytes [40] and chemical-induced neurons. In this latter case, β-actin deficiency is linked to loss of chromatin-binding of Brg1, an ATPase of the BAF chromatin remodeling complex. This leads to defects in heterochromatin marks and impaired expression of neuronal gene programs [41].

Whether PC6.3 cells undergo profound changes in their global chromatin organization is not known at the moment, but our RNA-seq analysis revealed 1338 genes that displayed altered expression (Log2FC > 1 or < -1) during PC6.3 cell differentiation. Functional annotation of these genes reflects the cellular processes that are known to take place during differentiation: decreased proliferation and increased plasma membrane remodeling for neurite outgrowth (Fig. 2B). Whether increased nuclear actin is required to elicit these changes in gene expression is not known. In several other experimental systems, modulation of nuclear actin levels have been linked to regulation of MRTF/SRF target gene expression [16–18]. Hence it was not too surprising that we observed down-regulation of MRTF/SRF transcription activity (Fig. 2E) and target gene expression (Fig 2A, C-D) during later stages of PC6.3 cell differentiation, when increased nuclear actin was also observed. Mechanistically, this down-regulation of MRTF/SRF is achieved by controlling MRTF-A nuclear localization, which was markedly decreased during differentiation (Fig. 4E–F). Interestingly, regulation of MRTF subcellular localization in neuronal cells seems to be more complex and cell type-specific than in fibroblasts, where this process has been extensively studied. In some neuronal cells, MRTF-A has been shown to shuttle between the cytoplasm and the nucleus, whereas in cortical and hippocampal neurons, exclusively nuclear localization has been reported [28]. It has been hypothesized that due to the mostly nuclear MRTF-A localization in some cells, nuclear actin would modulate MRTF-A expression rather than localization [42]. However, in our PC6.3 cell model, MRTF-A protein levels do not change upon differentiation (Fig. 4B), and MRTF-A shows both cytoplasmic and nuclear distributions (Fig. 4C, E), which seem similar to the actin-dependent nucleo-cytoplasmic shuttling characterized in fibroblasts [11].

Importantly, before the decreased activity of MRTF/SRF after days with NGF, the pathway is transiently activated during the first hours of applying the differentiation conditions (Fig. 3). Activation of MRTF/SRF downstream of NGF has been shown already before [16,43], and several studies have reported the requirement for MRTF/SRF target gene expression during neuronal differentiation and function. For example, expression of dominant-negative MRTF constructs inhibits neuronal outgrowth and guidance [44] and depletion of MRTFs by RNAi reduces dendritic complexity [45]. Moreover, lack of both MRTFs in mice leads to disruption of multiple brain areas with defects in neuronal migration and neurite outgrowth [46]. In addition, expression of actin mutants in either cytoplasm or nucleus regulates neuronal motility in SRF-dependent manner [42]. Since MRTF/SRF regulate the expression of numerous cytoskeletal target genes, defects in cellular processes that are driven especially by actin dynamics are therefore not surprising, and early activation of MRTF/SRF during neuronal differentiation is logical.

It is, however, less obvious why MRTF/SRF activity decreases later during differentiation. It might be that this is merely a specific feature of the used cell model, and reflects the conditions used to stimulate differentiation by low serum containing media. On the other hand, a recent study utilizing reprogramming of somatic cells to induced pluripotent stem cells has suggested that SRF can repress expression of cell-type specific genes through their epigenetic regulation [47]. Perhaps SRF inactivation is required also in the PC6.3 cells to allow expression of genes required for neuronal differentiation. An important caveat of our RNA-seq analysis is that MRTF/SRF target genes have not been firmly established in neurons. We used a target gene list from fibroblasts derived from MRTF-A chromatin-binding patterns and sensitivity to actin-binding drugs [23]. Target genes are often cell-type specific, due to, for example, partnership with different transcription factors. Overall, further studies are needed to establish MRTF/SRF target genes in different cellular contexts.

4. Materials and methods

4.1. Plasmids

GFP-actin plasmid is described in Ref. [2]

4.2. Antibodies

The following antibodies were from Thermo Scientific: GAPDH (MA5-15738, 1:2500), the following ones from Merck: Anti-Actin AC-40 (A3853, 1:1000), tubulin (T6074, 1:2500) and nucleolin (N2662, 1:1000). SRF (5147, 1:750), MRTF-A (14760S, 1:1000) and cofilin (3312, 1:1000) antibodies were from Cell Signaling Technology, Ipo9 (PAB0154, 1:1000) from Abnova and MRTF-A G8 (sc-390 324, 1:50) from Santa Cruz Biotechnology. Phospho-Ser3 cofilin antibody (11 139–1, 1:1000) was from Signalway antibody. The following secondary antibodies were from Thermo Fisher Scientific: horseradish peroxidase (HRP) conjugated anti-mouse IgG (G-21040, 1:5000), HRP-conjugated anti-rabbit IgG (G-21234, 1:5000) and Alexa-Fluor-488 conjugated anti-mouse IgG (A11001, 1:500).

4.3. Cell lines, differentiating cells and transfections

PC6.3 cells obtained from Urmas Arumäe (Tallinn University of Technology) were cultured in RPMI-1640 medium (Lonza) supplemented with 10% horse serum (HS; Gibco), 5% fetal bovine serum (FBS; Gibco), penicillin-streptomycin (Thermo Fisher Scientific) and GlutaMAX (Thermo Fisher Scientific) in 5% CO_2 incubator at + 37 °C. For differentiation, cells were plated on poly-L-lysine (Merck) and laminin (Merck) coated cell culture plates in full RPMI medium. Next day, medium was replaced to low serum RPMI (RPMI-1640 supplemented with 1% HS and 1% FBS) with 50 ng/ml NGF 2.5S Native Mouse Protein (Gibco) to differentiate cells for desired time. Control cells were kept in low serum RPMI without NGF during the duration of the experiment. For GFP-actin transfection, differentiating PC6.3 cells were transfected using JetPrime transfection reagent (Polyplus) according to manufacturer's protocol using total DNA amount of 250 ng per 24 well plate well/1000 ng per 35 mm dish out of which 25% was GFP-actin and the rest filled with pEF-Flag plasmid.

4.4. Nuclear/cytosol fractionation

PC6.3 cells were plated to 10 cm cell culture plates at densities 500 000–1 000 000 cells per plate, differentiated for 0–5 days and nuclei were separated from the cytoplasm using Nuclear/Cytosol Fractionation Kit (BioVision) according to manufacturer's instructions. SDS-PAGE loading buffer was added to resulting fractions and the samples were processed for SDS-PAGE and Western blot using anti-Actin Ac-40, anti-tubulin and anti-nucleolin antibodies to verify the performance of the fractionation and to study actin distribution during differentiation. Intensities of bands were measured with Fiji ImageJ software, actin in cytoplasmic and nuclear fractions normalized to tubulin and nucleolin, respectively, and data presented as nuclear to cytoplasmic actin ratio.

4.5. Immunofluorescence and microscopy

PC6.3 cells were plated on 24 well cell culture plates with coverslips at a density of 5000–10 000 cells per well. Cells were differentiated for 0–8 h or for 0–5 days for MRTF-A staining and for 0–5 days for GFP-actin transfection. The transfection was done one day before fixation. Before fixation, relief phase images were taken with FLoid Cell Imaging Station (Thermo Scientific) using a fixed 20x plan fluorite objective to confirm that cells were differentiated. Cells were fixed with 4% paraformaldehyde for 20 min, washed three times with PBS and permeabilized with 0.1% Triton X-100 (Merck) in PBS for 5 min. Samples were then blocked in blocking buffer [1% gelatin (Merck), 1% BSA (Merck), 10% FBS (Lonza) in PBS] for 30 min and mounted in Prolong Diamond with DAPI (Thermo Scientific), or stained with primary antibody MRTF-A G8 diluted in blocking buffer for 45 min, washed and stained with secondary Alexa Fluor-488 antibody for 45 min. Coverslips were washed in PBS and in MilliQ and mounted as above.

Imaging was done using Zeiss LSM 700 confocal with Axio Imager M2 microscope, ZEN 2012 software and LCI Plan-Neofluar 63x/1.30 Imm Corr glycerol objective. Fixed samples were imaged to analyze MRTF-A or GFP-actin distribution in cells. Imaging was done using 405 nm (for DAPI) and 488 nm (for Alexa Fluor-488 or GFP) lasers, the pinhole was set to 1 AU, resolution was 668x668 and bit depth 8. Fluorescence intensities were measured from cell nucleus and cytoplasm using Fiji ImageJ software and the ratios were calculated by dividing the average nuclear intensity with cytoplasmic intensity.

4.6. Total protein amounts during differentiation

PC6.3 cells were plated on 6 well cell culture plates at a density of 80 000 cells per well and differentiated with NGF for 0–5 days. Differentiated cells were lysed to 1x SDS-PAGE loading buffer and samples were processed for SDS-PAGE and Western blotting using anti-Actin AC-40, MRTF-A (Cell Signaling Technology), SRF, Ipo9, cofilin, phospho-cofilin and GAPDH antibodies. Intensities of bands were measured with Fiji ImageJ software and normalized to GAPDH.

4.7. Luciferase assay

Cells were plated on 24 well cell culture plates at a density of 100 000 cells per well and differentiated with NGF for 0–8 h or 0–4 days. Cells were transfected with SRF reporter p3DA.luc (8 ng per well) and reference reporter pTK-RL (20 ng per well) by JetPrime transfection reagent. Total DNA amount was 200 ng per well, and the rest was filled with pEF-myc plasmid. For 0 and 8 h differentiated cells, the transfection was done the day before NGF stimulation. For 0–4 days differentiated cells, the transfection was done one day before the assay. After differentiation was completed, Dual-Luciferase reporter assay system (Promega) kit was used according to manufacturer's instructions to measure the relative SRF reporter activity. For data analysis, the activity of firefly luciferase was normalized to renilla luciferase activity.

4.8. FLIP

PC6.3 cells were plated on 35 mm cell culture dishes at a density of 80 000 cells per dish and differentiated for 0–3 days as previously. During the last day before imaging, cells were transfected with GFP-actin. Next day, cells were live imaged in +37 °C, 5% CO_2 in Okolab bold line cage incubator using Zeiss LSM 700 confocal with Axio Imager M2 microscope with W Plan-Apochromat 63x/1.0 dipping objective. Acquisition software was ZEN 2012. Imaging parameters: pinhole 1 AU,

resolution 256x256, bit depth 12, speed 7, line average 1, zoom 2. The cytoplasm was continuously bleached for 120 s with 2 s intervals using 100% laser power (488 nm/10 mW) and the loss of fluorescence in the nucleus resulting from export of GFP-actin to the cytoplasm was recorded. Bleaching was started after 3 scans. Data was processed by setting the pre-bleach values to 1 and by producing a linear fit of the first data points to get the export rate.

4.9. FRAP

PC6.3 cells were plated on 35 mm glass bottom cell culture dishes at a density of 80 000 cells per dish and differentiated for 0–3 days as previously. During the last day before imaging, cells were transfected with GFP-actin. Next day, cells were live imaged in +37 °C, 5% CO_2 in LifeImagingSystems incubation system using Leica TCS SP5 II HCS-A confocal with DMI6000 B microscope with HCX PL APO 63x/1,2 W Corr/0,17 CS water objective, RSP 500 beam splitter and FRAPbooster. Acquisition software was LAS AF 2.7.7. Imaging parameters: pinhole 1 AU, resolution 256x256, bit depth 12, speed 700 Hz, bidirectional X scan, line average 2 and zoom 6, resulting in 0.374 s per frame. Laser power (Ar 488/35 mW) was set to 80% and 4% was used for imaging. After two pre-bleach images, a circle with a diameter of 4 μm in the nucleus was bleached with 100% laser power with the zoom in option. The recovery was followed as fast as possible for the first 30 s and then at 2 s intervals. The data was analyzed by setting the pre-bleach values to 1 and by producing a linear fit of the first data points to get the import rate.

4.10. RNA-seq

For RNA-seq, PC6.3 cells were plated to 6 well cell culture plates and differentiated for 0–5 days. Total RNA was extracted with a Nucleospin RNA kit from Macherey-Nagel according to the manufacturer's protocol from quadruplicates. Libraries were prepared for Illumina NextSeq 500 using Ribo-Zero rRNA Removal Kit (Illumina) and the NEBNext Ultra Directional RNA Library Prep at the Biomedicum Functional Genomics Unit (FuGU) according to the manufacturer's protocols. RNA-seq data sets were aligned using TopHat2 (using Chipster software) to version Rnor_6.0 of the Rattus norvegicus genome with the default settings. Counting aligned reads per genes were performed with HTSeq. Differential expression analysis and Principal components analysis (PCA) were performed with DESeq. List of the transcribed genes was based on cutoff >10 of baseMean parameter for aligned reads counts of all RNA-seq. Gene ontology was performed using DAVID 6.8. RNA-seq data will be available at Gene Expression Omnibus with accession number GSE206781.

4.11. RT-qPCR

PC6.3 cells were plated on 6 well cell culture plates at a density of 80 000 cells per well and differentiated with NGF for 0–8 h or for 0–5 days. RNA was extracted using the NucleoSpin RNA kit (Macherey-Nagel) according to the manufacturer's instructions. cDNA was made from 250 ng of RNA using Maxima First Strand cDNA Synthesis Kit for RT-qPCR (Thermo Scientific) and 1:10 diluted cDNA was used for qPCR. qPCR was done with SensiFAST SYBR No-ROX Kit master mix (Meridian Bioscience) using the following primers:

Primers for RT-qPCR.

Target	Orientation	Sequence (5′ to 3′)
Actb	Forward	AGATCAAGATCATTGCTCCTCCT
Actb	Reverse	ACGCAGCTCAGTAACAGTCC
Gapdh	Forward	AAGGTCATCCCAGAGCTGAA
Gapdh	Reverse	CTGCTTCACCACCTTCTTGA
Ipo9	Forward	GGAGGTGACAGAGGAATTTGG
Ipo9	Reverse	CTCTGATTGGGCACACCAGT
Srf	Forward	AGACGGGCATCATGAAGAAG
Srf	Reverse	GTCTCACTGGTGATCATGGG
Vcl	Forward	TGGTCTAGCAAGGGCAATGA
Vcl	Reverse	CTCGTCACCTCATCAGAGGC
Xpo6	Forward	CGGTACTTACGCCAGAGCT
Xpo6	Reverse	CTGTGTCCTGACCCCGAAG

(continued on next column)

(continued)

Relative expression levels were calculated by the comparative Ct method, normalizing to Gapdh.

4.12. Statistical analyses

Statistical analyses were performed in Origin 2021b. Normality was tested and when data conformed to a normal distribution, two-tailed one-sample or two-sample *t*-test was performed. When data was not normally distributed, a two-tailed Mann-Whitney test was used. All statistical tests were done with the significance level of 0.05. The used statistical test is indicated in the figure legends.

Kyheröinen et al. Credit author statement

Salla Kyheröinen: Conceptualization; Investigation; Visualization; Writing – original draft, Alise Hyrskyluoto: Conceptualization; Investigation, Maria Sokolova: Conceptualization; Formal analysis; Data Curation; Writing – original draft, Maria K. Vartiainen: Conceptualization; Writing – original draft; Supervision; Funding acquisition.

Declarations of competing interest

None

Data availability

GEO code is in the materials and methods for RNA-seq data

Acknowledgements

We thank Paula Maanselkä for excellent technical assistance. This work was supported by Sigrid Juselius, Cancer and Jane and Aatos Erkko foundations, Academy of Finland grants 338281 and 330254 to MKV, as well as Academy of Finland grant 308890 to AH and Instrumentarium Science foundation grant to SK. Imaging was performed at the Light Microscopy Unit, Institute of Biotechnology and RNA-seq at Biomedicum Functional Genomics Unit, both supported by HiLIFE and Biocenter Finland.

Appendix A. Supplementary data

Supplementary data to this article can be found online at https://doi.org/10.1016/j.yexcr.2022.113356.

References

[1] S. Ulferts, B. Prajapati, R. Grosse, M.K. Vartiainen, Emerging properties and functions of actin and actin filaments inside the nucleus, Cold Spring Harbor Perspect. Biol. 13 (2021).
[2] J. Dopie, K.P. Skarp, E. Kaisa Rajakyla, K. Tanhuanpaa, M.K. Vartiainen, Active maintenance of nuclear actin by importin 9 supports transcription, Proc. Natl. Acad. Sci. U. S. A. 109 (2012) E544–E552.
[3] T. Stuven, E. Hartmann, D. Gorlich, Exportin 6: a novel nuclear export receptor that is specific for profilin.actin complexes, EMBO J. 22 (2003) 5928–5940.
[4] K.P. Skarp, G. Huet, M.K. Vartiainen, Steady-state nuclear actin levels are determined by export competent actin pool, Cytoskeleton (Hoboken) 70 (2013) 623–634.

[5] V.A. Spencer, S. Costes, J.L. Inman, R. Xu, J. Chen, M.J. Hendzel, M.J. Bissell, Depletion of nuclear actin is a key mediator of quiescence in epithelial cells, J. Cell Sci. 124 (2011) 123–132.

[6] A. Fiore, V.A. Spencer, H. Mori, H.F. Carvalho, M.J. Bissell, A. Bruni-Cardoso, Laminin-111 and the level of nuclear actin regulate epithelial quiescence via exportin-6, Cell Rep. 19 (2017) 2102–2115.

[7] H.Q. Le, S. Ghatak, C.Y. Yeung, F. Tellkamp, C. Gunschmann, C. Dieterich, A. Yeroslaviz, B. Habermann, A. Pombo, C.M. Niessen, S.A. Wickstrom, Mechanical regulation of transcription controls Polycomb-mediated gene silencing during lineage commitment, Nat. Cell Biol. 18 (2016) 864–875.

[8] M.T. Bohnsack, T. Stuven, C. Kuhn, V.C. Cordes, D. Gorlich, A selective block of nuclear actin export stabilizes the giant nuclei of Xenopus oocytes, Nat. Cell Biol. 8 (2006) 257–263.

[9] M. Feric, C.P. Brangwynne, A nuclear F-actin scaffold stabilizes ribonucleoprotein droplets against gravity in large cells, Nat. Cell Biol. 15 (2013) 1253–1259.

[10] Y.Z. Xu, T. Thuraisingam, D.A. Morais, M. Rola-Pleszczynski, D. Radzioch, Nuclear translocation of beta-actin is involved in transcriptional regulation during macrophage differentiation of HL-60 cells, Mol. Biol. Cell 21 (2010) 811–820.

[11] M.K. Vartiainen, S. Guettler, B. Larijani, R. Treisman, Nuclear actin regulates dynamic subcellular localization and activity of the SRF cofactor MAL, Science 316 (2007) 1749–1752.

[12] S. Mouilleron, C.A. Langer, S. Guettler, N.Q. McDonald, R. Treisman, Structure of a pentavalent G-actin*MRTF-A complex reveals how G-actin controls nucleocytoplasmic shuttling of a transcriptional coactivator, Sci. Signal. 4 (2011) ra40.

[13] R. Pawlowski, E.K. Rajakyla, M.K. Vartiainen, R. Treisman, An actin-regulated importin alpha/beta-dependent extended bipartite NLS directs nuclear import of MRTF-A, EMBO J. 29 (2010) 3448–3458.

[14] C. Baarlink, H. Wang, R. Grosse, Nuclear actin network assembly by formins regulates the SRF coactivator MAL, Science 340 (2013) 864–867.

[15] M. Plessner, M. Melak, P. Chinchilla, C. Baarlink, R. Grosse, Nuclear F-actin formation and reorganization upon cell spreading, J. Biol. Chem. 290 (2015) 11209–11216.

[16] M.R. Lundquist, A.J. Storaska, T.C. Liu, S.D. Larsen, T. Evans, R.R. Neubig, S. R. Jaffrey, Redox modification of nuclear actin by MICAL-2 regulates SRF signaling, Cell 156 (2014) 563–576.

[17] M. Chatzifrangkeskou, D.E. Pefani, M. Eyres, I. Vendrell, R. Fischer, D. Pankova, E. O'Neill, RASSF1A is required for the maintenance of nuclear actin levels, EMBO J. 38 (2019), e101168.

[18] S. Marco, M. Neilson, M. Moore, A. Perez-Garcia, H. Hall, L. Mitchell, S. Lilla, G. R. Blanco, A. Hedley, S. Zanivan, J.C. Norman, Nuclear-capture of endosomes depletes nuclear G-actin to promote SRF/MRTF activation and cancer cell invasion, Nat. Commun. 12 (2021) 6829.

[19] M.C. McNeill, J. Wray, G.B. Sala-Newby, C.C.T. Hindmarch, S.A. Smith, R. Ebrahimighaei, A.C. Newby, M. Bond, Nuclear actin regulates cell proliferation and migration via inhibition of SRF and TEAD, Biochim. Biophys. Acta Mol. Cell Res. 1867 (2020), 118691.

[20] J. Zhou, J.S. Valletta, M.L. Grimes, W.C. Mobley, Multiple levels for regulation of TrkA in PC12 cells by nerve growth factor, J. Neurochem. 65 (1995) 1146–1156.

[21] T.F. Dijkmans, L.W. van Hooijdonk, T.G. Schouten, J.T. Kamphorst, A.C. Vellinga, J.H. Meerman, C.P. Fitzsimons, E.R. de Kloet, E. Vreugdenhil, Temporal and functional dynamics of the transcriptome during nerve growth factor-induced differentiation, J. Neurochem. 105 (2008) 2388–2403.

[22] K.H. Lee, C.J. Ryu, H.J. Hong, J. Kim, E.H. Lee, CDNA microarray analysis of nerve growth factor-regulated gene expression profile in rat PC12 cells, Neurochem. Res. 30 (2005) 533–540.

[23] C. Esnault, A. Stewart, F. Gualdrini, P. East, S. Horswell, N. Matthews, R. Treisman, Rho-actin signaling to the MRTF coactivators dominates the immediate transcriptional response to serum in fibroblasts, Genes Dev. 28 (2014) 943–958.

[24] A.V. Leopold, K.G. Chernov, A.A. Shemetov, V.V. Verkhusha, Neurotrophin receptor tyrosine kinases regulated with near-infrared light, Nat. Commun. 10 (2019) 1129.

[25] R.N. Pittman, S. Wang, A.J. DiBenedetto, J.C. Mills, A system for characterizing cellular and molecular events in programmed neuronal cell death, J. Neurosci. 13 (1993) 3669–3680.

[26] B. Offermann, S. Knauer, A. Singh, M.L. Fernandez-Cachon, M. Klose, S. Kowar, H. Busch, M. Boerries, Boolean modeling reveals the necessity of transcriptional regulation for bistability in PC12 cell differentiation, Front. Genet. 7 (2016) 44.

[27] A. Eggert, N. Ikegaki, X. Liu, T.T. Chou, V.M. Lee, J.Q. Trojanowski, G.M. Brodeur, Molecular dissection of TrkA signal transduction pathways mediating differentiation in human neuroblastoma cells, Oncogene 19 (2000) 2043–2051.

[28] B. Knoll, Actin-mediated gene expression in neurons: the MRTF-SRF connection, Biol. Chem. 391 (2010) 591–597.

[29] K.P. Skarp, M.K. Vartiainen, Actin as a model for the study of nucleocytoplasmic shuttling and nuclear dynamics, Methods Mol. Biol. 1042 (2013) 245–255.

[30] A. Hyrskyluoto, M.K. Vartiainen, Regulation of nuclear actin dynamics in development and disease, Curr. Opin. Cell Biol. 64 (2020) 18–24.

[31] N. Nusser, E. Gosmanova, Y. Zheng, G. Tigyi, Nerve growth factor signals through TrkA, phosphatidylinositol 3-kinase, and Rac1 to inactivate RhoA during the initiation of neuronal differentiation of PC12 cells, J. Biol. Chem. 277 (2002) 35840–35846.

[32] T. Yan, Z. Zhang, D. Li, NGF receptors and PI3K/AKT pathway involved in glucose fluctuation-induced damage to neurons and alpha-lipoic acid treatment, BMC Neurosci. 21 (2020) 38.

[33] G.X. Shi, D.A. Andres, Rit contributes to nerve growth factor-induced neuronal differentiation via activation of B-Raf-extracellular signal-regulated kinase and p38 mitogen-activated protein kinase cascades, Mol. Cell Biol. 25 (2005) 830–846.

[34] J. Xing, J.M. Kornhauser, Z. Xia, E.A. Thiele, M.E. Greenberg, Nerve growth factor activates extracellular signal-regulated kinase and p38 mitogen-activated protein kinase pathways to stimulate CREB serine 133 phosphorylation, Mol. Cell Biol. 18 (1998) 1946–1955.

[35] N.L. Klages-Mundt, A. Kumar, Y. Zhang, P. Kapoor, X. Shen, The nature of actin-family proteins in chromatin-modifying complexes, Front. Genet. 9 (2018) 398.

[36] M. Sokolova, H.M. Moore, B. Prajapati, J. Dopie, L. Merilainen, M. Honkanen, R. C. Matos, M. Poukkula, V. Hietakangas, M.K. Vartiainen, Nuclear actin is required for transcription during Drosophila oogenesis, iScience 9 (2018) 63–70.

[37] P. Therizols, R.S. Illingworth, C. Courilleau, S. Boyle, A.J. Wood, W.A. Bickmore, Chromatin decondensation is sufficient to alter nuclear organization in embryonic stem cells, Science 346 (2014) 1238–1242.

[38] S.R. Mahmood, X. Xie, N. Hosny El Said, T. Venit, K.C. Gunsalus, P. Percipalle, beta-actin dependent chromatin remodeling mediates compartment level changes in 3D genome architecture, Nat. Commun. 12 (2021) 5240.

[39] T. Gjorgjieva, X. Xie, P. Commins, R. Pasricha, S.R. Mahmood, K.C. Gunsalus, P. Naumov, P. Percipalle, Loss of beta-actin leads to accelerated mineralization and dysregulation of osteoblast-differentiation genes during osteogenic reprogramming, Adv. Sci. 7 (2020), 2002261.

[40] M.A. Al-Sayegh, S.R. Mahmood, S.B.A. Khair, X. Xie, M. El Gindi, T. Kim, A. Almansoori, P. Percipalle, beta-actin contributes to open chromatin for activation of the adipogenic pioneer factor CEBPA during transcriptional reprograming, Mol. Biol. Cell 31 (2020) 2511–2521.

[41] X. Xie, R. Jankauskas, A.M.A. Mazari, N. Drou, P. Percipalle, beta-actin regulates a heterochromatin landscape essential for optimal induction of neuronal programs during direct reprograming, PLoS Genet. 14 (2018), e1007846.

[42] S. Stern, E. Debre, C. Stritt, J. Berger, G. Posern, B. Knoll, A nuclear actin function regulates neuronal motility by serum response factor-dependent gene transcription, J. Neurosci. 29 (2009) 4512–4518.

[43] S.R. Wickramasinghe, R.S. Alvania, N. Ramanan, J.N. Wood, K. Mandai, D. D. Ginty, Serum response factor mediates NGF-dependent target innervation by embryonic DRG sensory neurons, Neuron 58 (2008) 532–545.

[44] B. Knoll, O. Kretz, C. Fiedler, S. Alberti, G. Schutz, M. Frotscher, A. Nordheim, Serum response factor controls neuronal circuit assembly in the hippocampus, Nat. Neurosci. 9 (2006) 195–204.

[45] M. Ishikawa, N. Nishijima, J. Shiota, H. Sakagami, K. Tsuchida, M. Mizukoshi, M. Fukuchi, M. Tsuda, A. Tabuchi, Involvement of the serum response factor coactivator megakaryoblastic leukemia (MKL) in the activin-regulated dendritic complexity of rat cortical neurons, J. Biol. Chem. 285 (2010) 32734–32743.

[46] M.H. Mokalled, A. Johnson, Y. Kim, J. Oh, E.N. Olson, Myocardin-related transcription factors regulate the Cdk5/Pctaire1 kinase cascade to control neurite outgrowth, neuronal migration and brain development, Development 137 (2010) 2365–2374.

[47] T. Ikeda, T. Hikichi, H. Miura, H. Shibata, K. Mitsunaga, Y. Yamada, K. Woltjen, K. Miyamoto, I. Hiratani, Y. Yamada, A. Hotta, T. Yamamoto, K. Okita, S. Masui, Srf destabilizes cellular identity by suppressing cell-type-specific gene expression programs, Nat. Commun. 9 (2018) 1387.